Intracellular Drug Delivery Using Low-Frequency Ultrasound: Quantification of Molecular Uptake and Cell Viability

Keyvan Keyhani,[1] Héctor R. Guzmán,[1] Aimee Parsons,[1] Thomas N. Lewis,[2,3] and Mark R. Prausnitz[1,4]

Received May 25, 2001; accepted August 3, 2001

Purpose. To determine the dependence on acoustic parameters of molecular uptake and viability of cells exposed to low-frequency ultrasound.

Methods. DU145 prostate cancer cells bathed in a solution of calcein were exposed to ultrasound at 24 kHz over a range of different acoustic pressures, exposure times, pulse lengths, and duty cycles. Flow cytometry was employed to quantify the number of calcein molecules delivered into each cell and levels of cell viability.

Results. Both molecular uptake and cell viability showed a strong dependence on acoustic pressure and exposure time, weak dependence on pulse length, and no significant dependence on duty cycle. When all of the data were pooled together, they exhibited good correlation with acoustic energy exposure. Although molecular uptake showed large cell-to-cell heterogeneity, up to ~15% of cells achieved an intracellular calcein concentration approximately equal to its extracellular concentration.

Conclusions. Large numbers of molecules can be delivered intracellularly using low-frequency ultrasound. Both uptake and viability correlate with acoustic energy, which is useful for design and control of ultrasound protocols.

KEY WORDS: ultrasound; drug delivery; cavitation; sonophoresis.

INTRODUCTION

The success of drug and gene delivery is limited by the inability of drugs, proteins, and DNA to cross biological barriers in the body. The most daunting barrier is that posed by lipid bilayers, which block transport into cells (e.g., the plasma membrane), into tissues (e.g., tumors), and into the body (e.g., skin, mucosa). To overcome this barrier, ultrasound has been shown to dramatically increase the permeability of cell membranes and tissues to small compounds and macromolecules (1–3). Because it can be focused noninvasively on almost any part of the body (4), ultrasound has the potential to be a platform technology useful for enhanced and targeted delivery for a broad range of indications.

Previous studies have demonstrated ultrasound's utility for a number of different drug- and gene-delivery applications. Early *in vitro* studies have demonstrated increased drug efficacy when accompanied by ultrasound (5). Ultrasound has also been shown to increase DNA transfection in cell suspensions and in animals (1,6,7). Ultrasound has further been applied to the skin to increase transdermal transport (2) and, more recently, used to extract interstitial glucose transdermally from human subjects (8). Limited work has shown that ultrasound can increase transport across the blood–brain barrier (9).

Although exciting applications of ultrasound have been demonstrated, there is limited information available to guide selection of appropriate or optimal ultrasound conditions. The goal of this study is to address this need by measuring how acoustic pressure, exposure duration, pulse length, duty cycle, and energy each affect ultrasound's ability to increase uptake of molecules into cells and associated loss of cell viability.

Ultrasound's effects are believed to be caused primarily by ultrasound-induced cavitation (10,11). Ultrasound is an oscillating pressure wave that can bring dissolved gas out of solution during low pressure, thereby creating bubbles. During subsequent pressure oscillations, these bubbles can grow, oscillate and implode, which can have violent effects on cells. Ultrasonic imaging safely utilizes conditions in which cavitation does not occur and therefore does not damage tissues. In contrast, lithotripsy focuses acoustic energy to shatter kidney stones by creating extensive local cavitation. Ultrasound-mediated drug delivery seeks middle ground, where sufficient cavitation is generated to permeabilize cell membranes to drugs and/or genes, but not so much cavitation that there is excessive loss of cell viability.

MATERIALS AND METHODS

Cell Sample Preparation

As described by Guzman *et al.* (3), DU145 human prostate cancer cells (American Type Culture Collection, Rockville, MD) were cultured as monolayers in a humidified atmosphere of 95% air and 5% CO_2 at 37°C in RPMI-1640 media, supplemented with 10% (v/v) heat inactivated fetal bovine serum, and 100 μg/mL penicillin-streptomycin (Cellgro, Mediatech, Herndon, VA). Cells were harvested by trypsin/EDTA (Cellgro) digestion, washed, and resuspended at a concentration of 5×10^5 cells/mL in cell media containing 10 μM calcein (623 Da, radius = 0.6 nm; Molecular Probes, Eugene, OR). Calcein is a green-fluorescent, cell-impermeant molecule that was used to quantify transport of molecules into viable cells.

Prior to ultrasound exposure, cell samples were filled into a sample tube prepared by cutting a 15-mL polypropylene centrifuge tube (VWR, Suwanee, GA) at the 4 mL line. After the sample tube was filled with cell suspension, a rubber stopper (VWR) was carefully inserted into the tube to the 3 mL line, thereby spilling out a small amount of suspension. This procedure was used so that the tube could be sealed without any entrapped air bubbles. A metal rod was also inserted through a small hole in the center of the rubber stopper to facilitate positioning the sample at the axial and

[1] School of Chemical Engineering, Georgia Institute of Technology, Atlanta, Georgia 30332–0100.
[2] George W. Woodruff School of Mechanical Engineering, Georgia Institute of Technology, Atlanta, Georgia 30332-0405.
[3] Present address: Center on Human Development and Disability, University of Washington, Seattle, Washington 98195-7920.
[4] To whom correspondence should be addressed. (e-mail: mark.prausnitz@che.gatech.edu)

0724-8741/01/1100-1514$19.50/0

radial center of the transducer within the ultrasound exposure chamber.

Exposure to Ultrasound

As described by Liu *et al.* (12), the ultrasound exposure chamber consisted of a cylindrical piezoelectric transducer sandwiched between two 10-cm lengths of PVC pipe. The chamber was sealed at its base and filled with filtered, deionized, degassed water. The sample tube was placed within the ultrasound exposure chamber water bath and exposed to low-frequency (24 kHz) ultrasound at room temperature (22 ± 2°C).

To characterize ultrasound exposures, peak incident pressure was determined using a calibrated hydrophone as described previously (12). Ultrasound usually was applied in a pulsed manner, where the pulse length indicates the duration of "on" time during each pulse, duty cycle indicates the ratio of "on" time to the sum of "on" time and "off" time between each pulse, and exposure time indicates the total "on" time over all pulses during an exposure. For example, if 100 pulses each of 10-ms duration were applied with 90-ms gaps of "off" time between each pulse, the pulse length would be 10 ms, the duty cycle would be 10%, and the exposure time would be 1 s. Energy exposure was calculated as $E = P^2t / 2\rho c$ (11), where P is rms pressure, t is time, ρ is density of water, and c is speed of sound in water.

Measurement of Molecular Uptake and Cell Viability

As described by Guzman *et al.* (3), cell samples were washed to remove calcein present in the extracellular fluid and subsequently incubated for at least 10 min in phosphate-buffered saline containing 0.1 mg/mL red-fluorescent propidium iodide (Molecular Probes) to stain non-viable cells. Fluorescent reference beads (Molecular Probes) were added to facilitate cell viability analysis as described previously (13).

A FACSort flow cytometer (Becton Dickinson, Franklin Lakes, NJ) was used to quantify molecular uptake and cell viability, as described by Guzman *et al.* (14). Forward and side scatter were used to distinguish cells from debris and reference beads. Green fluorescence of calcein was converted into the average number of calcein molecules delivered per cell using quantitative calibration beads (Flow Cytometry Standards Corporation, Fishers, IN). Red fluorescence of propidium iodine was used to distinguish viable from non-viable cells. MiX 3.1 statistical software (Ichthus Data Systems, Hamilton, Ontario, Canada) was used to divide cell populations into their three subpopulations, as discussed below.

At each condition tested, a minimum of three replicate data points were collected and are presented as means with their standard errors. A two-tailed Student's *t* test ($\alpha = 0.05$) was used when comparing two experimental conditions. When comparing three or more experimental conditions, a one-way analysis of variance was used ($\alpha = 0.05$). A value of $P < 0.05$ was considered statistically significant.

Restricted cubic splines (S-Plus, MathSoft, Seattle, WA) were used to identify trends in experimental data. The "goodness" of fit for each trend was measured using the multiple R^2 statistic, which relates the amount of variability in the response variable to that given by the fitted variable. A multiple R^2 of 1 indicates a perfect relationship between the fit and response variables, whereas a multiple R^2 of 0 indicates no relationship.

RESULTS

To guide design and optimization of ultrasound parameters useful for drug delivery, we used flow cytometry to measure molecular uptake and viability of DU145 prostate cancer cells as a function of ultrasound pressure, exposure duration, pulse length, duty cycle, energy, and timing of exposure.

Heterogeneity of Ultrasound's Effects on Cells

As observed in other studies (14,15), ultrasound's effects on cells are heterogeneous. Figure 1 contains a representative set of histograms that show the distribution of calcein uptake among large populations of viable cells each exposed to the same ultrasound conditions. Some cells show very little, if any, uptake, whereas others take up millions of molecules per cell. For this reason, we did not report the uptake associated with each ultrasound exposure as a single value. Instead, we divided each population of cells into three subpopulations (14), as shown graphically in Fig. 1C. The lower peak corre-

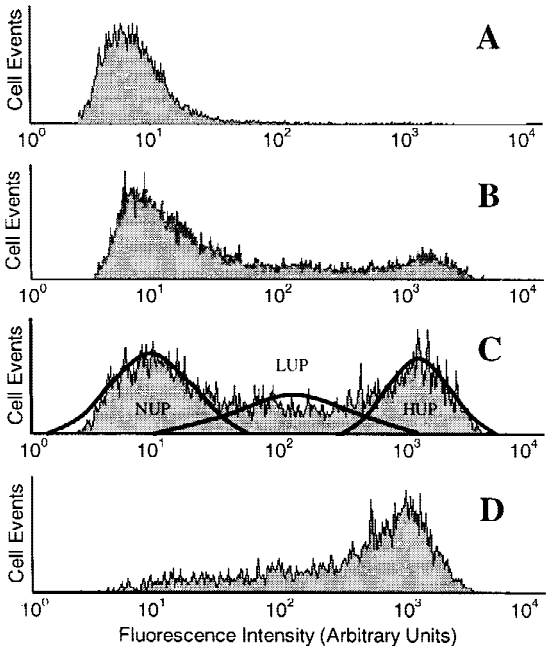

Fig. 1. Representative histograms of the number of calcein molecules taken up by prostate cancer cells. In (A), a control population of cells shows a single peak at low fluorescence due to system noise. In (B–D), progressively greater pressures result in brighter fluorescence, which corresponds to greater uptake of calcein into cells: (B) pressure, P = 5.3 atm; exposure time, τ = 0.5 s; energy, E = 6.9 J/cm^2; (C) P = 4.5 atm; τ = 2 s; E = 19.2 J/cm^2; (D) P = 8.0 atm, τ = 2 s; E = 62.1 J/cm^2; (B–D) pulse length, t = 100 ms; duty cycle, d = 10%. These uptake histograms show significant heterogeneity with a typical profile containing a peak at low fluorescence (nominal uptake), a peak at high fluorescence (high uptake), and a broad distribution in between (low uptake). These complex distributions have been characterized by fitting three Gaussian subpopulations to each histogram (illustrated in C) and reporting the fraction of cells and the average number of molecules per cell within each subpopulation (14).

sponds to nominal uptake (NUP), the higher peak corresponds to high uptake (HUP), and the broad distribution in between corresponds to low uptake (LUP) subpopulations. NUP cells are identified as having "nominal" uptake because their fluorescence is only slightly greater than that of control cells ($P < 0.05$) or, in some cases, indistinguishable from controls ($P > 0.05$).

Although the relative number of cells in each uptake subpopulation varied drastically as a function of ultrasound conditions, the average number of molecules within each subpopulation was generally of the same order of magnitude. For all of the ultrasound conditions tested (see below), the average number of molecules taken up by cells in each subpopulation was NUP = 1.5 ($\pm$ 2.1) $\times 10^5$, LUP = 2.7 ($\pm$ 1.2) $\times 10^6$, and HUP = 1.0 ($\pm$ 0.5) $\times 10^7$. For this reason, the data presented throughout this study characterize the degree of uptake by reporting the fraction of cells within each subpopulation.

Quantitative Dependence of Ultrasound's Effects on Ultrasound Parameters

Acoustic pressure is one of the critical parameters that controls ultrasound's effects on cells. Figure 2A shows the effects of pressure on both cell viability and molecular uptake among viable cells. The height of each bar represents cell viability, which decreases with increasing pressure (ANOVA; $P < 0.001$). Non-viable cells typically represent a mixture of intact cells (~20%) and cells fragmented into debris (~80%) (data not shown). The subdivisions within each bar represent the distribution of cells among the three uptake subpopulations. The fraction of NUP cells decreases with increasing pressure (ANOVA; $P < 0.001$). In contrast, the fraction of LUP and HUP cells increases, goes through a maximum, and then decreases with increasing pressure. This indicates that there is an optimal pressure that maximizes uptake.

Exposure time also influences ultrasound's effects on cells. Figure 2B shows that as exposure time increases, cell viability decreases (ANOVA; $P < 0.001$), the fraction of NUP cells also decreases (ANOVA; $P < 0.001$), and cells in the LUP and HUP go through a maximum. This behavior is similar to that seen for acoustic pressure and indicates that there is an optimal exposure time that maximizes uptake.

The effects of pulse length were less significant (Fig. 2C). Pulses of 1 ms in duration and shorter were somewhat more benign, yielding higher viabilities (Student's t test $P < 0.05$). This transition at approximately 1 ms may be due to cavitation bubble dynamics, as discussed elsewhere (15,16). As seen

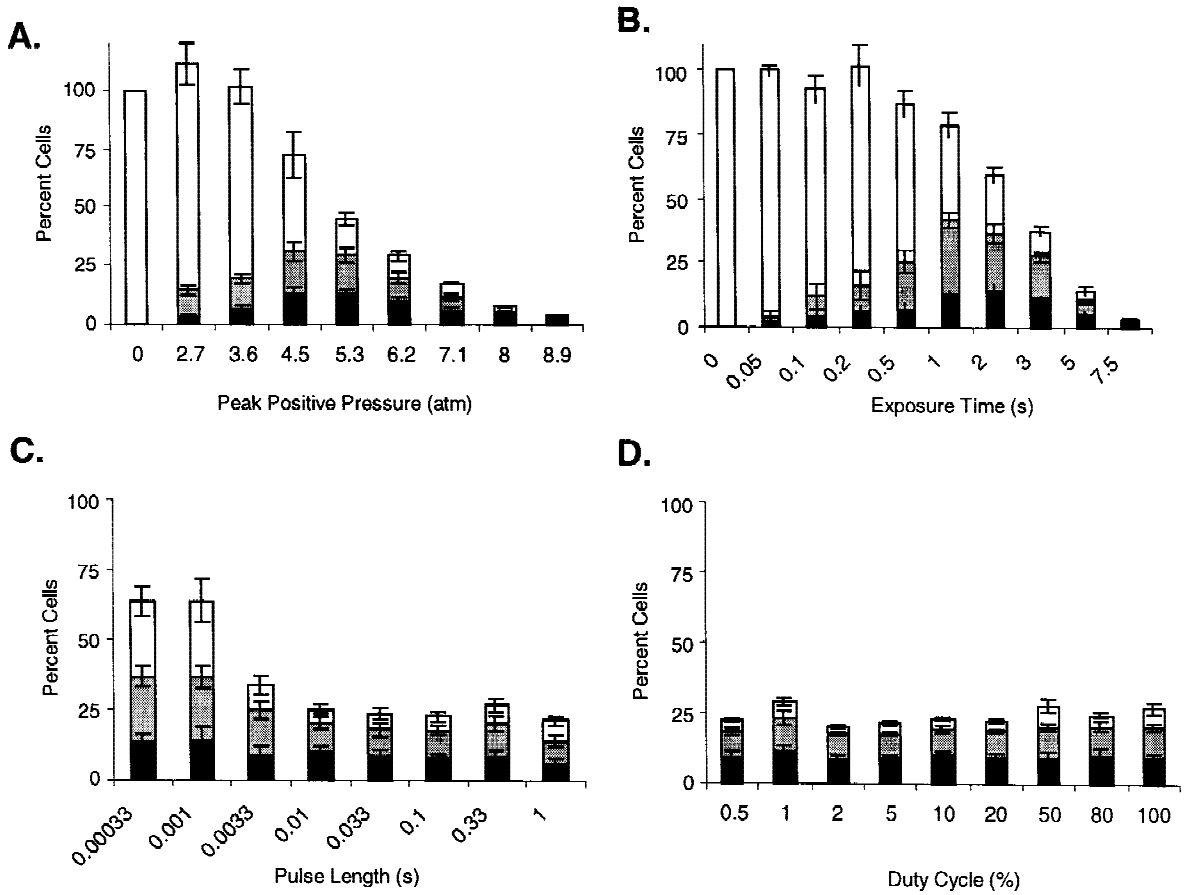

Fig. 2. Effects of ultrasound on cell viability and molecular uptake as functions of (A) ultrasound pressure (τ = 2 s; t = 100 ms; d = 10%), (B) exposure time (P = 5.3 atm; t = 100 ms; d = 10%), (C) pulse length (P = 6.2 atm; τ = 2 s; d = 10%), and (D) duty cycle (P = 6.2 atm; τ = 2 s; t = 100 ms). The height of each bar represents the percent of viable cells, whereas the stripes represent the fraction of cells in each subpopulation: high uptake (black), low uptake (gray), and nominal uptake (white).

in Figure 2D, there were no statistically significant effects caused by changing duty cycle (ANOVA; $P > 0.10$).

For some applications, it is important to know the fate of all cells treated with ultrasound; Figure 2 provides that type of information. However, for other applications, it may not matter how many cells are killed and only the fate of those cells remaining viable is important. For example, *in vitro* or *ex vivo* gene-transfer applications may need to yield a uniform population of transfected viable cells, even if a large fraction of cells are killed in the process. To address this scenario, Figure 3 shows the data from Figure 2 re-plotted such that the cells in the three uptake subpopulations are expressed as a fraction of viable cells (as opposed to fractions of all cells, shown in Fig. 2). In this case, uptake is optimized among the viable cells by using high pressures and long exposure times (ANOVA; $P < 0.05$). There is again a weak dependence on pulse length with a transition near 1 ms (Student's t test; $P = 0.007$–0.022). Duty cycle has no significant effect over the range of conditions tested (ANOVA; $P > 0.20$).

Broad Correlation of Ultrasound's Effects with Acoustic Energy

Although the data presented in the above figures provide useful information to help identify optimal ultrasound conditions, it would be of even greater utility to have a single acoustic parameter that correlated with uptake and viability for all of these data. Because acoustic pressure and exposure time were the dominant influences on ultrasound's effects on cells and because acoustic energy is proportional to exposure time and pressure squared, we tested the ability of energy to correlate with these bioeffects.

Figure 4A shows viability versus acoustic energy exposure for all of the data in this study (i.e., shown in Figs. 2 and 3). Although there is some scatter, there is a reasonable correlation between cell viability and energy (restricted cubic spline $R^2 = 0.81$), where viability is high at low energies and then decreases with increasing energy. Figure 4B shows the average number of molecules delivered into each cell within each subpopulation. As discussed earlier, levels of uptake within each subpopulation are generally of the same order of magnitude, although uptake among NUP and LUP cells increases with energy (ANOVA; $P < 0.001$) and uptake among NUP cells shows considerable scatter.

The fraction of cells within each subpopulation is plotted as a function of acoustic energy in Figures 5 and 6. Figure 5 represents these data as fractions of all cells treated (similar to Fig. 2) and Figure 6 represents the data as fractions of only the cells remaining viable after treatment (similar to Fig. 3). Again, the data shown in Figures 2 and 3 all collapse down to single curves in Figure 5 (restricted cubic spline $R^2 = 0.82$, 0.31, and 0.31 for NUP, LUP, and HUP, respectively) and

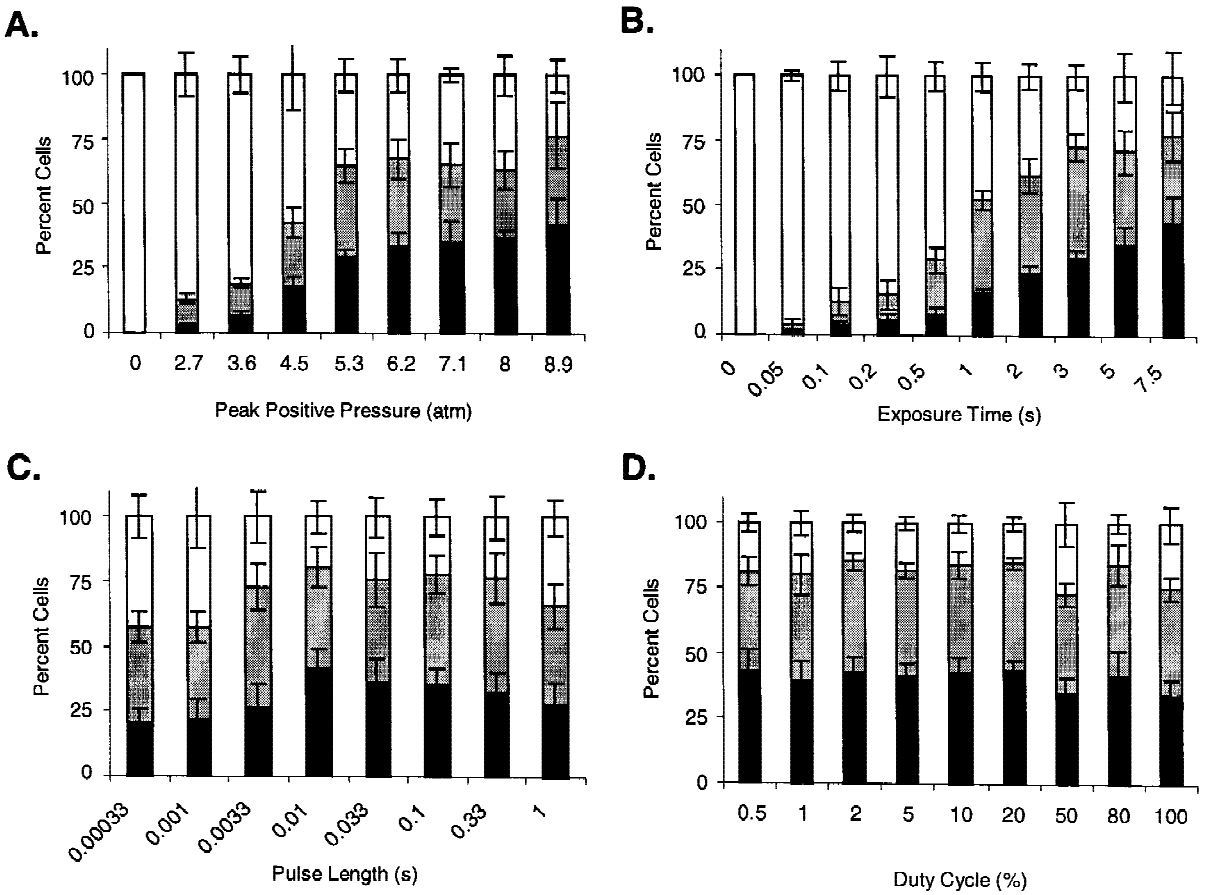

Fig. 3. Effects of ultrasound on molecular uptake among cells that remained viable as functions of (A) ultrasound pressure, (B) exposure time, (C) pulse length, and (D) duty cycle. The same data presented in Figure 2 are re-plotted to show the distribution of the three subpopulations among only the viable cells.

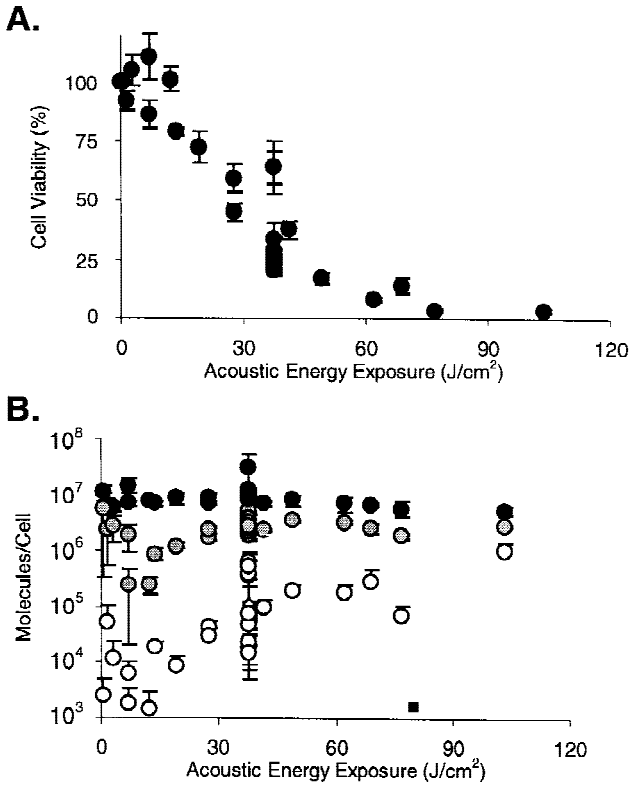

Fig. 4. Effects of ultrasound on (A) cell viability and (B) molecular uptake as functions of acoustic energy exposure. The data shown in Figure 2 have been reanalyzed and plotted here versus acoustic energy. Viability shows a good correlation with energy. Molecular uptake by cells in each of the subpopulations is generally of the same order of magnitude (see text).

Figure 6 (restricted cubic spline $R^2 = 0.62$, 0.50, and 0.62 for NUP, LUP, and HUP, respectively), indicating a broad correlation between molecular uptake and acoustic energy.

DISCUSSION

High Levels of Molecular Uptake

It is significant for drug- and gene-delivery applications that ultrasound can be used to deliver large numbers of molecules into viable cells. Cells in the HUP had an average of 1.0×10^7 molecules per cell. Based on a cell volume of 2200 ± 200 μm^3 (14), this corresponds to an intracellular concentration of 7.5 μM, which is close to the extracellular concentration of 10 μM. Thus, sonicated cells can internalize molecules at a level approaching thermodynamic equilibrium.

Despite very high levels of uptake by some cells, there is considerable heterogeneity. As much as 15% of treated cells can show the highest levels of uptake (HUP), and as much as 40% of cells can have some significant level of uptake (LUP + HUP); however, in most cases the majority of cells are either in the NUP subpopulation or are non-viable (Figs. 2 and 4). The cause of this heterogeneity is presently unclear but may be due to cell-to-cell differences or could result from non-uniformity in the cavitation field created by ultrasound. Although in some cases heterogeneity could be a limitation, in other cases it could be used as an asset, especially for targeting. For example, if some cells are more susceptible to ultrasound's effects, then those cells could be selectively loaded with drugs or genes. Alternatively, if non-uniform cavitation is the cause of heterogeneity, then targeted regions could be pre-seeded with cavitation nuclei (e.g., stabilized gas bubbles) to focus ultrasound's effects.

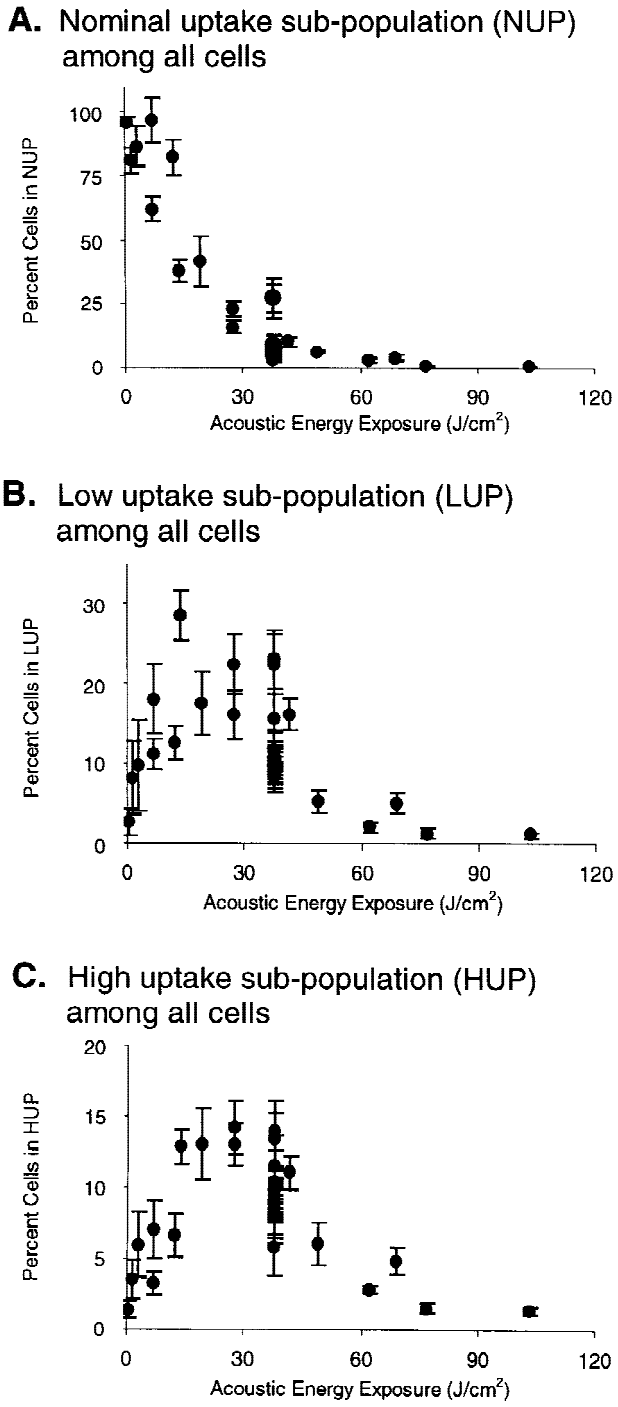

Fig. 5. Effects of ultrasound on cell distribution among the (A) nominal uptake, (B) low uptake, and (C) high uptake subpopulations shown as functions of acoustic energy exposure. The data shown in Figure 2 have been reanalyzed and plotted here versus acoustic energy. All of the data fall into a single curve on each graph, which indicates that energy is a good predictor of ultrasound's bioeffects. Optimization of the fraction of cells in the low uptake and/or high uptake subpopulations occurs at ~30 J/cm^2.

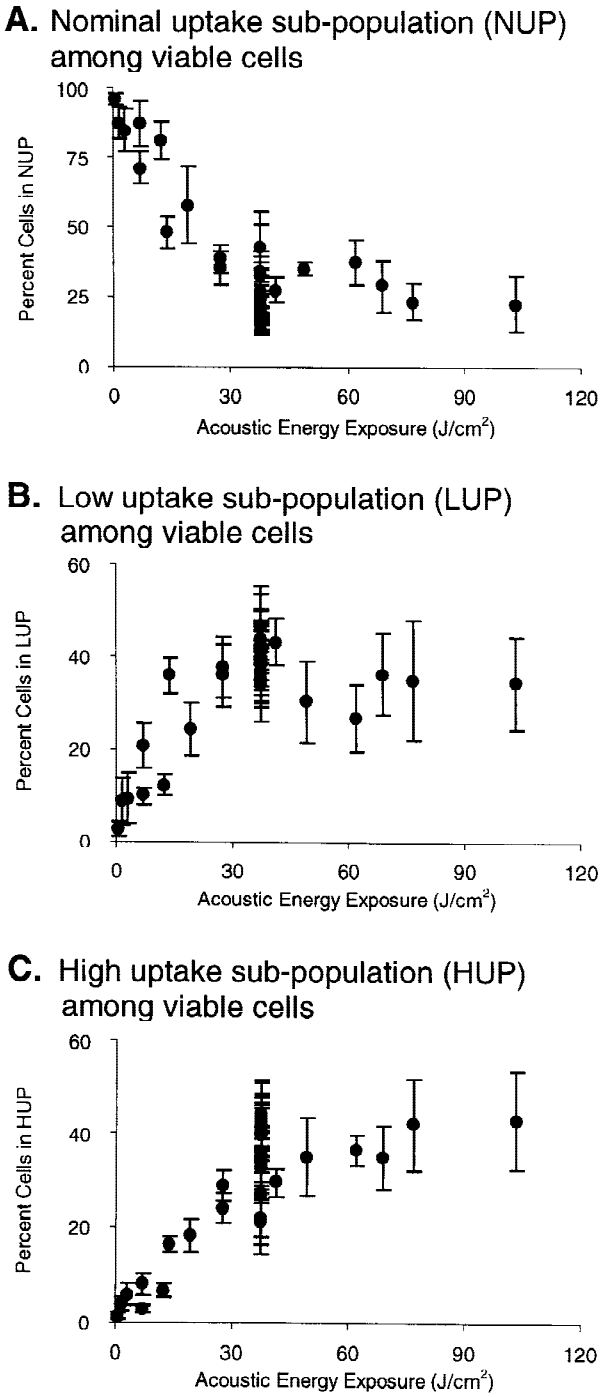

Fig. 6. Effects of ultrasound on the distribution of viable cells among the (A) nominal uptake, (B) low uptake, and (C) high uptake subpopulations shown as functions of acoustic energy exposure. The data shown in Figure 3 have been reanalyzed and plotted here versus acoustic energy. All of the data fall into a single curve on each graph, which indicates that energy is a good predictor of ultrasound's bioeffects. The fraction of viable cells in the low uptake and/or high uptake subpopulations increases with increasing energy.

Although the results of this study may be directly applied to *in vitro, ex vivo,* or other scenarios in which cells are in dilute suspension, applying its implications to *in vivo* effects of ultrasound on intact tissue are less straightforward. This is because the cell disruption studied here is believed to be mediated by creation, oscillation, and possible implosion of cavitation gas bubbles (10,11). In a dilute suspension of cells, growth of these bubbles to microns dimensions can easily occur. At the boundary between a fluid space and tissue, such as when targeting the endothelial layer of a blood vessel or the outer surface of skin, this may also be feasible. However, within tissue, where cell density is high and extracellular space is limited, bubble growth may be constrained, which could diminish ultrasound's effects.

Correlation with Acoustic Energy

The broad correlation of acoustic energy with both uptake and viability should greatly facilitate the process of developing and applying ultrasound protocols for different applications. First, having a single, easily measured parameter that correlates with bioeffects makes controlling an ultrasound device more straightforward. In addition, technical or other constraints may limit the range of ultrasound conditions that can be applied. Because energy is a function of both pressure and exposure time, many possible combinations of ultrasound conditions can yield the same energy and, thus, the same biologic effects. This means that if a therapy would benefit from rapid effects, then a short (e.g., sub-second), high-pressure burst of ultrasound can be applied. However, the hardware needed for high pressures is more costly. If longer exposures are acceptable, then less-costly hardware can be employed for longer, lower pressure ultrasound to achieve the same effect.

Figure 5 suggests that to induce uptake in the greatest number of cells, an acoustic energy exposure of approximately 30 J/cm^2 should be used. Although this number is almost certainly specific to our apparatus and possibly to our cell type, comparison with other literature studies may give insight. Guzman *et al.* (14) performed a similar study using the same cell type but a different apparatus that operated using 500-kHz ultrasound. In that study, molecular uptake was maximized at on the order of 100 J/cm^2, which is similar to the value determined here. Mitragotri *et al.* used ultrasound at a similar frequency to ours (20 kHz), but studied its effects on skin. They found that the onset of ultrasonic disruption of skin, as measured by electrical conductivity, occurred at ~10 J/cm^2 for rat skin *in vivo* (17) and ~200 J/cm^2 for pig skin *in vitro* (18), a range that brackets the values found for cells. Given the many physical and biologic differences between these studies, it is not clear that quantitative comparisons are meaningful. Nevertheless, it is worth noting that the energies of interest in these studies all fall within an order of magnitude of each other.

CONCLUSIONS

Ultrasound was shown to reversibly disrupt cell membranes and thereby deliver large numbers of molecules into viable cells. Within each sample, the number of molecules taken up by each cell was heterogeneous. Up to 40% of cells exhibited significant uptake and up to 15% achieved maximum intracellular concentrations in approximate thermodynamic equilibrium with the extracellular solution. The remaining cells were either unaffected or made non-viable. Both molecular uptake and cell viability strongly depended on pressure and exposure time, weakly on pulse length, and

insignificantly on duty cycle. All of the data were shown to correlate with acoustic energy exposure, which may serve as a single, predictive parameter. Because acoustic energy can be easily measured, this correlation may prove useful as a tool to design ultrasound protocols and to monitor or control them during application. Combined, these findings suggest that ultrasound can provide a non-invasive means for intracellular drug delivery.

ACKNOWLEDGMENTS

We thank Robert Karaffa for help with flow cytometry, and Robyn Schlicher, Jin Liu, Sohail Khan, Monali Desai, and Debalina Siddeeq for technical assistance. This work was supported in part by the National Science Foundation, The Whitaker Foundation and the National Institutes of Health.

REFERENCES

1. M. Fechheimer, J. F. Boylan, S. Parker, J. E. Sisken, F. L. Patel, and S. G. Zimmer. Transfection of mammalian cells with plasmid DNA by scrape loading and sonication loading. *Proc. Natl. Acad. Sci. USA* **84**:8463–8467 (1987).
2. S. Mitragotri, D. Blankschtein, and R. Langer. Ultrasound-mediated transdermal protein delivery. *Science* **269**:850–853 (1995).
3. H. R. Guzman, D. X. Nguyen, S. Khan, and M. R. Prausnitz. Ultrasound-mediated disruption of cell membranes I: Quantification of molecular uptake and cell viability. *J. Acoust. Soc. Am.* **110**:588–596.
4. F. W. Kremkau. *Diagnostic Ultrasound: Principles and Instruments*, W.B. Saunders, Philadelphia, PA, 1998.
5. A. H. Saad and G. M. Hahn. Ultrasound enhanced drug toxicity on chinese hamster ovary cells in vitro. *Cancer Res.* **49**:5931–5934 (1989).
6. J. A. Wyber, J. Andrews, and A. D'Emanuele. The use of sonication for the efficient delivery of plasmid DNA into cells. *Pharm. Res.* **14**:750–756 (1997).
7. P. G. Amabile, J. M. Waugh, T. N. Lewis, C. J. Elkins, W. Janas, and M. D. Dake. High-efficiency endovascular gene delivery via therapeutic ultrasound. *J. Am. Coll. Cardiol.* **37**:1975–1980 (2001).
8. J. Kost, S. Mitragotri, R. Gabbay, M. Pishko, and R. Langer. Transdermal monitoring of glucose and other analytes using ultrasound. *Nat. Med.* **6**:347–350 (2000).
9. J. T. Patrick, M. N. Nolting, S. S. Goss, K. A. Dines, J. L. Clendenon, M. A. Rea, and R. F. Heimburger. Ultrasound and the blood-brain barrier. *Adv. Exp. Med. Biol.* **267**:369–381 (1990).
10. S. B. Barnett, G. R. ter Haar, M. C. Ziskin, W. L. Nyborg, K. Maeda, and J. Bang. Current status of research on biophysical effects of ultrasound. *Ultrasound Med. Biol.* **20**:205–218 (1994).
11. T. G. Leighton. *The Acoustic Bubble*, Academic Press, London, 1994.
12. J. Liu, T. N. Lewis, and M. R. Prausnitz. Non-invasive assessment and control of ultrasound-mediated membrane permeabilization. *Pharm. Res.* **15**:920–926 (1998).
13. M. R. Prausnitz, B. S. Lau, C. D. Milano, S. Conner, R. Langer, and J. C. Weaver. A quantitative study of electroporation showing a plateau in net molecular transport. *Biophys. J.* **65**:414–422 (1993).
14. H. R. Guzman, D. X. Nguyen, S. Khan, and M. R. Prausnitz. Ultrasound-mediated disruption of cell membranes II: Heterogeneous effects on cells. *J. Acoust. Soc. Am.* **110**:597–606.
15. S. A. Cochran and M. R. Prausnitz. Sonoluminescence as an indicator of cell membrane disruption by acoustic cavitation. *Ultrasound Med. Biol.* **27**:841–850.
16. L. O. Kober, J. W. Ellwart, and H. Brettel. Effect of the pulse length of ultrasound on cell membrane damage in vitro. *J. Acoust. Soc. Am.* **86**:6–7 (1989).
17. S. Mitragotri, M. Coleman, J. Kost, and R. Langer. Transdermal extraction of analytes using low-frequency ultrasound. *Pharm. Res.* **17**:466–470 (2000).
18. S. Mitragotri, J. Farrell, H. Tang, T. Terahara, J. Kost, and R. Langer. Determination of threshold energy dose for ultrasound-induced transdermal drug transport. *J. Control. Release* **63**:41–52 (2000).